Impact of Wind Energy Integration on Grid Stability, Robustness and Management

BOUAZIZ LAILA, DHAOUI MEHDI, BEN HAMED MOUNA
Electrical Department,
University of Gabes,
National Engineering School of Gabes,
Zrig 6029,
TUNISIA

Abstract: - This work concerns the study of the impact of wind energy integration on the stability and management of the Tunisian electrical grid. The analysis is conducted using the PSS (Power System Simulation) in Matlab/Simulink (Model and simulate multidomain physical systems) software to assess the stability of a power grid that incorporates wind farms, utilizing various indicators of stability and robustness. The aim is to evaluate the stability of a test transmission grid (IEEE 9 bus) as well as the stability of the Tunisian grid both with and without a wind power plant, to identify the primary effects of this integration, and to estimate a maximum allowable penetration rate for the grid. This study is carried out through a series of dynamic simulations, introducing various disturbances into a model of the national grid. The results indicate that the integration rate of wind energy should not exceed 20% to maintain electrical parameters within acceptable limits and to avoid compromising the operational performance of the Tunisian grid.

Key-Words: - Wind energy, grid stability, inertia, rate of change of frequency, critical fault clearance Times, PSS toolbox, Stability, Robustness, IEEE 9-bus.

Received: May 13, 2024. Revised: October 22, 2024. Accepted: November 24, 2024. Published: December 31, 2024.

1 Introduction

Today, the utilization of renewable resources for electricity generation has become widespread across the globe. The rapid development of these energy sources can be attributed to potential environmental issues, the swift growth of the population (increased demand), and the depletion of fossil fuel reserves.

This expansion of renewable energy production within existing networks is not without its impacts. Therefore, it is essential to study these effects to ensure that the integration occurs without compromising the quality and performance of electrical networks. Conventional electricity generation primarily relies on large traditional synchronous machines, which, due to their physical characteristics and without additional investment, provide significant inertia to the electrical system, [1].

This inertia means that immediately following the loss of a substantial portion of electricity production, the resulting drop in system frequency is delayed by the inertia of all rotating masses. This delay is crucial, as several seconds pass before additional primary power reserves can be deployed to restore balance to the electrical system while remaining within acceptable frequency deviation limits.

From the perspective of the electrical system, the generation of electricity from renewable sources operates quite differently compared to conventional production facilities. In addition to their intermittent nature, most of these sources are connected to the grid through power electronic converters, which diminishes the overall inertia of the electrical system. This inertia is often regarded as a critical parameter for the synchronized operation of current electrical systems. Indeed, a lower level of inertia results in an increased rate of change of frequency (RoCoF), and the grid frequency becomes highly responsive to sudden shifts in production and load, [2], [3].

Furthermore, a sufficient level of grid robustness must be always maintained, regardless of whether the situation is normal or disturbed. Traditionally, this robustness has been represented by the available fault level at a specific node in the electrical grid in relation to the nominal value of a renewable energy source (RES) connecting to that node. The short-circuit ratio (SCR) has been utilized to assess the system's robustness at the interconnection point of the RESs. Connecting

RESs to nodes with low short-circuit power can lead to potential issues concerning stability and voltage quality.

This work is necessitated by the current context. It focuses on the study of the impacts resulting from the integration of renewable energies, primarily wind energy, into the electrical grid.

In accordance with the objectives set forth, this work is organized into two sections.

The first section will provide an overview of the scenarios and challenges associated with the integration of renewable energy sources globally. Following this, the stability and control of the electrical grid, both with and without the integration of renewable energy sources, will be introduced.

The second section will present and analyze various stability indicators and methods for assessing the robustness of the grid. Specifically, the stability of the IEEE 9-Bus test grid and its robustness (SCR) will be evaluated using PSS toolbox in the absence of renewable energy sources, and the impact of wind resources on stability indicators will be detailed at the conclusion, particularly regarding the critical clearing time (CCT), total system inertia (Hsys), and the rate of change of frequency (RoCoF).

2 Challenges of RES Penetration

The generation of electrical energy from renewable sources, such as photovoltaic and wind energy, is primarily contingent upon the availability of the primary resource (PV/wind), which exhibits intermittent characteristics. Certain case studies, such as wind farms in Denmark and photovoltaic plants installed in Germany, suggest that when penetration rates exceed 20% or 30%, stability issues may arise.

The high sensitivity of renewable energy-based power plants to network disturbances, such as voltage dips or frequency variations, often results in a disconnection from production during network incidents. This disconnection can impair the normal operation of the electrical system and exacerbate the imbalance between production and consumption.

The current trend is to keep this production connected to the grid even in the event of voltage or frequency fluctuations. Achieving such an operation requires the implementation of an advanced control system. Several research projects have demonstrated, through statistical analyses and field recordings that integrating renewable energy sources at levels between 20% and 30% can lead to the following issues, [4]:

- A loss of stability in the electrical system occurs due to its intermittent nature.
- They reduce the available reserves necessary for maintaining the balance of the electrical system.
- They complicate the reliability of the production schedule, primarily due to the unpredictable nature of their output.
- Unlike production facilities that utilize rotating machinery, renewable energy installations incorporate power electronics, which can lead to a decrease in the system's inertia.

2.1 Stability of the Grid

The grid stability in a high voltage is a characteristic of a power system that enables it to maintain an equilibrium state under normal operating conditions and to return to an acceptable equilibrium state after experiencing a disturbance. Stability can be categorized based on the nature of the disturbance: rotor angle stability, voltage stability, and frequency stability. Additionally, stability can be classified according to the origin and magnitude of the fault, distinguishing between small and large amplitude disturbances. In terms of evaluation time, stability can be classified as short-term or long-term, as illustrated in Figure 1.

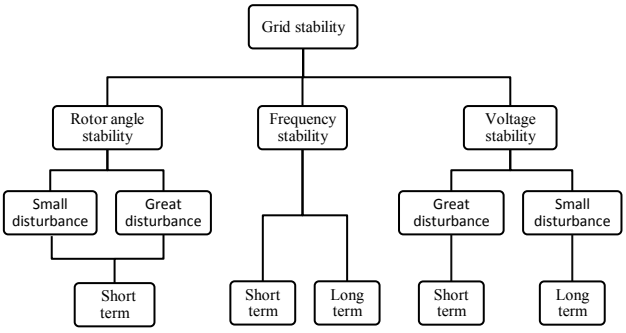

Fig. 1: Classification of grid stability

Disturbances can vary in magnitude, ranging from minor to significant. Minor disturbances, such as the rapid and continuous fluctuations in the production and transportation load of the system, occur regularly. The system adapts to these variations while maintaining an acceptable stability gradient and operational levels of voltage and frequency. In contrast, significant disturbances, such as the tripping of a generator or faults in transmission lines, result in substantial changes to the network topology and variations in the systems state parameters, including voltage and frequency.

The stability of electrical networks is a complex phenomenon that requires continuous monitoring by specialists to address and mitigate the impacts of

incidents and disturbances that may affect the electrical system. All advancements in stability problem resolution begin with an understanding of the disturbance scale, modeling the disturbance phenomena, and applying solutions through the art of mathematical simulation.

2.2 Grid Stability with the ERS Penetration

Conventional synchronous generators are unable to instantaneously adjust their output power to match load demands, resulting in a gradual acceleration or deceleration to address any shortfall until a change in speed occurs. This temporary alteration in power output leads to frequency variations, [4], [5].

The output from renewable energy sources fluctuates based on weather conditions, presenting a control challenge for the effective operation of the electrical system. Rapid changes in power generated by wind turbines, (which can reach several hundred kilowatts within a matter of seconds), along with load variations, can cause frequency fluctuations in the grid and trigger primary control adjustments of the rotating units. However, as long as the penetration rate of wind energy remains low, this variation can be regarded as negligible. Conversely, to ensure grid stability, it will be necessary to consider the participation of wind turbines in primary frequency control, with solutions that still require further investigation. If production exceeds consumption, the frequency will surpass the nominal value of 50Hz, and in such a situation, wind turbines must curtail their output. Most electrical systems possess adequate inertia in rotating machines to accommodate minor fluctuations in load. However, as the integration of renewable energy sources increases, these fluctuations are likely to become more significant, and the reserve capacity of synchronous machines may not be sufficient to manage them. Therefore, it is essential to implement measures to ensure that the impact of these variations on the frequency of the electrical system remains within the normal operating limits of the system, [6].

The new generation of large variable-speed wind turbines exhibits high moments of inertia due to their blades, which allow them to act as a filter for fluctuations in power and frequency. The rotating mass can also provide short-term frequency support to the electrical system. Long-term frequency support can be achieved by utilizing synchronous generators in conjunction with storage technologies such as fuel cells. These approaches fall under the category of primary frequency control. Additional frequency control relies on maintaining balancing reserves and implementing effective control systems.

Renewable energy systems that are electrically isolated typically connect to the grid through a power electronic converter, which is designed to monitor the grid frequency and adjust its output accordingly. Additional control is crucial for photovoltaic systems that lack inertia. Power electronic converters play a vital role in facilitating the interface between renewable generation and the grid, aiming to enhance the stability gradient of the frequency, [7].

2.3 Electric Grid Control

The purpose of electric grid control is to restore a state of operational equilibrium following a physical disturbance. Most variables and performance indicators of the electrical system, such as frequency, voltage, and angle, are maintained within permissible limits to ensure the normal operation of the electrical system. Consequently, the primary control loops are referred to as frequency control, voltage control, and rotor angle control. In numerous electrical networks, advanced measurement devices such as Phasor Measurement Units (PMUs) and modern communication systems have already been installed. These devices enable the adjustment of parameters for existing electrical system controls through an online control mechanism that relies on real-time data. The data obtained from PMUs is utilized to estimate critical parameters of the system. Subsequently, these parameters are incorporated into the control algorithm, which modifies the controller settings for frequency, voltage, and power oscillation regulation. As a result, the controller parameters are tailored to reflect the current state of the system.

3 Control Requirements

3.1 Requirements for Voltage Control

Wind and photovoltaic power plants are required to continuously, dynamically, and rapidly participate in the voltage control of the transmission network. They must be equipped with an automatic voltage regulation system and be capable of supplying or absorbing the reactive power necessary to maintain voltage within the acceptable operating limits of the transmission network under steady-state conditions. Voltage regulation in a wind or photovoltaic power plant can be achieved either by the wind turbine itself or through other equipment such as synchronous compensators or STATCOMs. Under

normal operating conditions of the transmission network, a wind or photovoltaic power plant must not generate rapid voltage fluctuations at the connection point exceeding ± 5% of the nominal voltage. Standards establish ranges for normal and abnormal operating voltages. Specifically, for each mode of operation, a minimum operating period is specified. These specifications are detailed in Table 1.

Table 1. Accepted voltage ranges

Voltage interval	Minimum operating period
0.80 U_n - 0.85 U_n	30 min
0.85 U_n - 0.93 U_n	3 h
0.93 U_n - 1.07 U_n	Unlimited
1.07 U_n - 1.10 U_n	1 h
1.10 U_n - 1.20 U_n	15 min

3.2 Requirements for Frequency Control

For normal operating frequencies (49.5 Hz - 50.5 Hz), renewable energy production facilities connected to high and medium-voltage grid must remain continuously connected to the grid while operating within the parameters for active and reactive power for which they were designed, like conventional power plants. Frequencies are categorized into normal and abnormal operating ranges, each associated with specific minimum operating durations. The frequency ranges and their corresponding operating durations are detailed in Table 2.

Table 2. Accepted frequency ranges

Frequency interval (Hz)	Minimum operating period
47.5 - 48.5	The cumulative duration is 15 minutes over the lifespan of the installation.
48.5 - 49.5	Continuous operation for 5 hours, with a cumulative duration of 100 hours throughout the lifespan of the installation
49.5 - 50.5	Unlimited
50.5 - 51	Continuous operation for 1 hour, with a cumulative duration of 15 hours during the lifespan of the installation
51 - 52	15 minutes, occurring once to five times per year

3.3 Requirements of Active Power Generation

Production units utilizing renewable energy sources must be controllable in terms of active power to mitigate risks to the grid or disturbances in system balance. Under normal operating conditions, a wind or photovoltaic power plant must be capable of:

- Adjusting the rate of increase or decrease of the produced active power to the value specified by the control center (MW/minute).
- Reducing the produced active power, upon instruction from the control center to the required level while adhering to the established rate of variation (charging/discharging).

4 Stability and Robustness Indicators

This section will examine the impact of integrating wind turbines into an IEEE 9-Bus test network. The first part will define various stability indicators: the critical clearing time (CCT), the inertia of power systems (H), and the rate of change of frequency (RoCoF).

Subsequently, three methods for assessing the robustness of the network will be outlined (SCR, WSCR, and CSCR), followed by an evaluation of transient stability, frequency stability, and the robustness of the IEEE 9-Bus network. Finally, an analysis of the effect of wind turbine penetration on the stability indicators will be conducted to highlight the significance of the interconnection point's rigidity of the renewable energy source with the grid and the inertia of the latter, [5].

4.1 Stability Indicators

4.1.1 Critical Clearing Time (CCT)

To ensure transient stability, any fault within the electrical system must be cleared promptly to keep the system within its stability limits. The critical clearing time (CCT) is the most widely used criterion for assessing the transient stability of an electrical system. It represents the maximum duration that a disturbance can be sustained without causing the system to lose synchronism and stability. A decrease in the CCT indicates a reduction in the transient stability margin of the system. The fault must be cleared by the protection mechanism before the critical time is reached. Consequently, the operational range of CCT values can be established based on the protection scheme. Indeed, the critical fault clearance time must exceed the clearing time required by the protection equipment, plus an additional safety margin. Typically, CCT values range from 100 ms to 1s.

The fault clearance time is determined for a specific disturbance and fault duration by analyzing the variations in the relative angles of synchronous generators. The rotor angle of one of the network generators (usually the generator at the balancing node) is used as a reference. The variations in the different relative angles (α_i) are compared to a

reference angle (α_r) set at ± 180°. When $|\alpha_i| > |\alpha_r|$, the generator(s) meeting this condition are deemed unstable, [6].

4.1.2 Inertia of Power Systems

In the grid, the rotational speed of the machines connected to the grid is directly associated with the frequency at their terminals. The total mechanical inertia stored in these machines provides not only a form of resistance to changes in their rotational speed but also inherently opposes any alterations in frequency. Consequently, the inertia of these machines is regarded as a crucial parameter essential for the synchronized operation of contemporary electrical systems. Conventional generators store kinetic energy within their rotating components. This stored energy is either released or absorbed in response to a disturbance. The expression for the kinetic energy of a synchronous generator is provided by:

$$E_k = \frac{1}{2}.J.\Omega^2 \quad (1)$$

where J represents the moment of inertia of the rotating mass in kg·m², and Ω denotes the angular velocity of the shaft in rad/s.

Kinetic energy changes when a power/torque imbalance is imposed on the system. Therefore, we can establish a relationship between the equilibrium of active power within the system and the deviation of the rotor speed.

$$P_m(t) - P_e(t) = \frac{dE_k}{dt} \approx \Omega_0.J\frac{d\Omega}{dt} \quad (2)$$

where, Ω_0 represents the nominal angular velocity of the shaft, measured at 314 rad/s, P_m and P_e denotes the mechanical and electrical power in megawatts (MW).

To quantify and highlight the inertia of a machine, the parameter H is utilized. This represents the inertia constant, measured in seconds, which indicates the duration in seconds that a generator can deliver its rated power solely by utilizing the kinetic energy (E_k) stored in its rotating mass. This inertia constant can be defined as the ratio of the system's kinetic energy to the nominal apparent power (S) of synchronous machines, [8], [9].

$$H = \frac{E_k}{S} \approx \Omega_0.J.\frac{d\Omega}{dt} \quad (3)$$

To illustrate the relationship between active power balance and the inertia constant H, the moment of inertia J in relation (1) is substituted into equation (2).

$$P_m(t) - P_e(t) = \frac{2.H.S}{\Omega_0}.\frac{d\Omega}{dt} \quad (4)$$

The oscillation equation (4) is expressed in per unit (p.u) as follows:

$$P_m(t)\check{}P_e(t) = 2.H.\frac{d\Omega}{dt} = 2.H.\frac{df}{dt} \quad (5)$$

By examining equation (5), it can be concluded that the inertia of a synchronous machine, represented by its inertia constant H, reflects the resistance to a change in frequency that arises from an imbalance between mechanical power and electrical power.

In an electrical network, each synchronous machine operates at the same frequency under steady-state conditions. When a significant power imbalance occurs, each generator will exhibit distinct oscillatory movements around the center of inertia (COI), influenced by the disparity between its mechanical and electrical power. However, all machines will ultimately synchronize to achieve the same speed through control and synchronization mechanisms. Consequently, these machines can be consolidated into a single unit, with their mechanical behavior governed by a singular oscillation equation expressed in per unit as follows:

$$2.H_{sys}.\frac{df_{coi}}{dt} = P_G(t).P_L(t) = \Delta P \quad (6)$$

where, H_{sys} represents the total inertia constant of the system, f_{coi} denotes the frequency at the center of inertia, and P_G and P_L indicates the total generated and load powers.

The inertia of the system is not a constant parameter, as the number and type of machines connected to the network fluctuate over time.

The equivalent inertia of the entire set of rotating machines also referred to as system inertia, is defined as the weighted sum of the inertia constants of each connected machine.

$$H_{sys} = \frac{\sum_{i=1}^{n} H_i.S_i}{S_{sys}} \quad (7)$$

S_{sys} represents the total capacity for synchronous production, while *n* denotes the number of synchronous machines connected to the system. Frequency instability may result in frequency oscillations, which can trigger the activation of production units or loads if the frequency exceeds a specific range or if the rate of change of frequency (RoCoF) becomes excessively high.

4.1.3 Rate of Change of Frequency (RoCoF)

The rate of change of frequency represents the time derivative of the electrical system's frequency (df/dt). This metric is crucial for assessing the resilience of an electrical grid and serves as a significant parameter for evaluating frequency stability. The instantaneous value of RoCoF

immediately following a power imbalance is equivalent to its value in the vicinity of zero, prior to any control actions being implemented.

$$R_o C_o F = \frac{df_{coi}}{dt}|_{t=0} = \frac{\Delta P}{2.H_{sys}} \quad (8)$$

According to relation (8), it is observed that the two key factors influencing the rate of frequency variation are the relative amount of power imbalance and the total inertia of the system at the time of the disturbance.

In Figure 2, the frequency as a function of time is presented for a power imbalance of 0.1 per unit. It illustrates that for a given imbalance, the frequency drop is significantly greater and occurs more rapidly when the inertia is reduced. Therefore, with a lower system inertia H_{sys}, the governor control must respond more promptly to prevent the frequency from declining to critical levels.

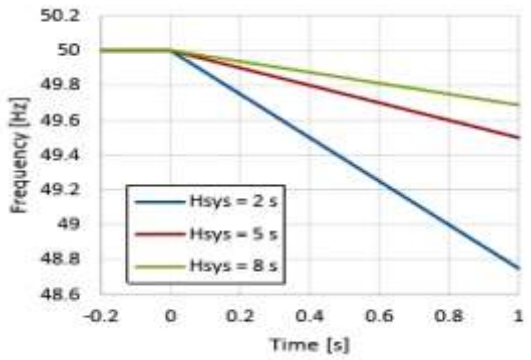

Fig. 2: Frequency evolution following a power imbalance of Δp=0.1 p.u, [7]

Figure 3 clearly indicates that for a power imbalance, the rate of change of frequency (RoCoF) decreases as the system's inertia increases.

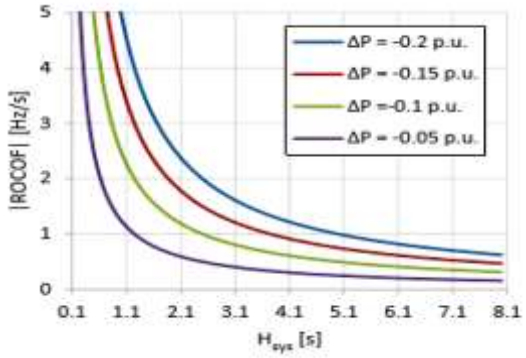

Fig. 3: Evolution of RoCoF in relation to the total inertia of the system

4.2 Evaluation of Grid Robustness

The robustness of the system was first defined by the AEMC in 2017 as follows: It is a characteristic of an electrical grid that relates to the magnitude of voltage variation resulting from a fault or disturbance within the grid.

The robustness of the system can be assessed by the availability of fault current at a specific location. High fault levels are typically observed in a robust electrical system, whereas low fault levels indicate a fragile electrical system. The resilience of the system is a shared concern in the integration of renewable energy sources. The performance of various components within an electrical system is contingent upon the system's robustness, which indicates how sensitive the system's variables are to different disturbances. When the network's resistance is high at a connection point, the voltage experiences minimal variation in response to changes in load or production. Conversely, when the system's robustness is lower, the voltage fluctuates more significantly for the same alteration.

The large-scale integration of renewable energy sources (RES) into an electrical system may alter the characteristics of the grid, particularly affecting voltage performance under normal operating conditions and potentially leading to undesirable issues related to stability and voltage quality. Therefore, it is essential to assess the robustness of the system at the connection points of the RES. To date, various methods have been developed to evaluate the system's resilience. However, each of these methods has its limitations and may not accurately represent the actual rigidity of the system at every interconnection point of the RES.

4.2.1 Short-Circuit Ratio (SCR)

The most employed method for assessing the network's stiffness at the interconnection point of the renewable energy sources (RES) is the Short-Circuit Ratio (SCR). This ratio indicates the rigidity of a bus within the network in relation to the rated power of a machine or an interconnected RES. The SCR is defined as the ratio of the short-circuit capacity S_{cci} (in MVA) at bus i, where the device is located, to the rated power of that device P_i (in MW).

$$SCR_i = \frac{S_{cci}}{P_i} \quad (9)$$

The calculated value of the System Strength Ratio (SCR) can be utilized to identify vulnerable areas within an electrical system, where enhanced compensation measures and monitoring are essential to address safety concerns. A robust system is characterized by an SCR exceeding three, while weak and very weak systems have SCR values

ranging from three to two and below two, respectively.

The traditional method for calculating SCR often overlooks the interactions among System Element Ratings (SERs), which may result in overly optimistic and inaccurate outcomes. To account for the impact of these interactions on system robustness, several improved methodologies have been developed, including the Weighted SCR (WSCR) proposed by ERCOT and the Composite SCR (CSCR) introduced by GE, [10], [11].

4.2.2 Weighted Short-Circuit Ratio (WSCR)

The WSCR provides a more accurate representation of the actual robustness of the system when a significant number of Renewable Energy Sources (RES) are integrated into an electrical system. This ratio is defined as the relationship between the weighted short-circuit capacity at the interconnection point of all RES within a specific area and their rated power.

$$WSCR = \frac{\sum_{i=1}^{N}(S_{cci}.P_i)}{\left(\sum_{i=1}^{N} P_i\right)^2} \quad (10)$$

where, S_{cci} represents the short-circuit capacity at bus i prior to the connection of the RES i, measured in MVA. Pi denotes the nominal power of the RES i to be connected, expressed in MW, and N indicates the total number of RES that are fully interacting with one another. This calculation method is predicated on the assumption of complete interactions among the RES within a specified area. It assumes that all RES are linked to a single Point of Interconnection (POI). In practical scenarios, there exists a certain electrical distance between the POIs, and not all RES interact completely with each other.

On the other hand, a minimum WSCR of 1.5 is required to ensure voltage stability and provide a certain margin of stability. The robustness of the system at the Point of Interconnection (POI) of the Renewable Energy Sources (RES), as calculated by the WSCR method, is significantly lower than that obtained through the SCR method. This indicates that renewable production sources interact with one another, resulting in a lower actual robustness of the system compared to the scenario where each source oscillates independently.

4.2.3 Composite Short-Circuit Ratio (CSCR)

The CSCR serves as a measure of the system's robustness, utilized to assess the ability of an electrical system to sustain stable operation when integrating sources reliant on power electronics converters. This ratio is defined as the relationship between the composite short-circuit capacity at the interconnection point of all Renewable Energy Sources (RES) within a specified area and their combined rated power.

$$CSCR = \frac{CompositeS_{cc}}{\sum_{i=1}^{N} P_i} \quad (11)$$

The composite short-circuit capacity is determined by selecting a bus within an electrical network that is near the interconnection point of the renewable energy sources (RES), thereby forming a composite bus. The short-circuit capacity is subsequently calculated at this bus.

Like the weighted short-circuit ratio (WSCR), the short-circuit ratio (CSCR) considers the impact of connecting multiple synchronous generators (SERs) in proximity. Typically, a robust system is characterized by a CSCR value ranging from approximately 2.5 to 3, whereas a fragile system exhibits a CSCR value between about 1.5 and 1.7, [6].

5 Stability and Robustness of the 9-Bus Test Grid

Test grid that complies with IEEE standards have been extensively utilized by researchers and engineers for various stability studies.

The electrical grids are constructed based on actual data in accordance with the standard IEEE electrical system configuration. In our work, we have selected the IEEE 9-Bus test grid. This test grid comprises three generators, three loads, and nine buses. The 9-Bus grid is modeled and simulated using the PSS toolbox in Matlab/Simulink. The single-line diagram is illustrated in Figure 4.

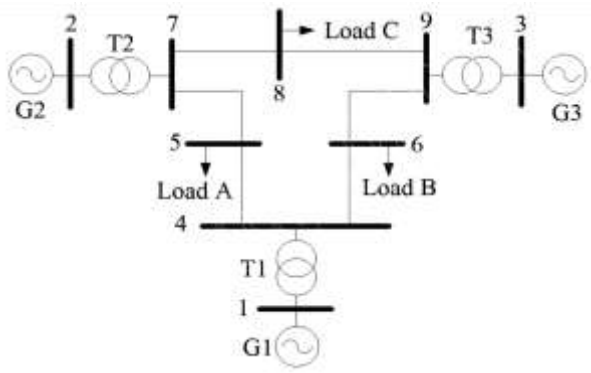

Fig. 4: Single-line diagram of the 9-Bus test grid

5.1 Load Flow Resolution

The stability study cannot be conducted without understanding the unknown variables related to the load flow of the grid prior to the fault.

To resolve this, numerous algorithms have been developed to take the issue of nonlinear load flows. Among these, the Gauss-Seidel and Newton-Raphson methods are commonly employed for load flow analysis and are readily available in all major electrical grid analysis software.

In most instances, engineers prefer the Newton-Raphson method due to its guaranteed convergence properties, [11].

The key information derived from the study of power/load flow includes the amplitudes and phase angles of bus voltages, as well as the active and reactive power of transmission lines and generator buses.

Figure 5 presents the resolution of load flow using the PSS toolbox, providing a detailed visualization of the computed power flow parameters.

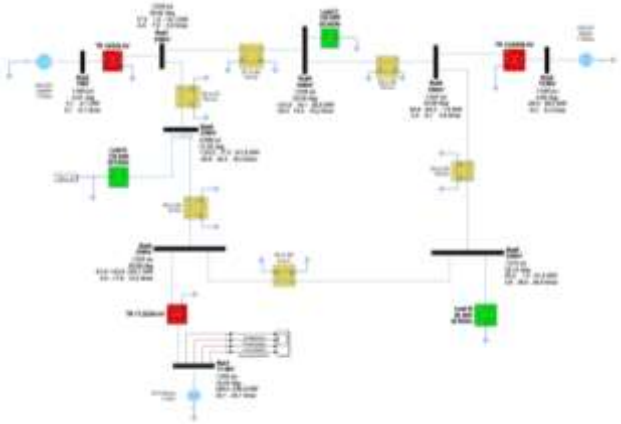

Fig. 5: Resolution of load flow using PSS toolbox

Table 3. Single-line diagram of the 9-Bus test grid

Bus	Type	P_{Gen}	Q_{Gen}	P_{ch}	Q_{ch}	U	α
		MW	MVAR	MW	MVAR	p.u	deg
1	**PV**	71.641	27.04	0	0	1.04	-9.28
2	**Swing**	163	6.65	0	0	1.02	0
3	**PV**	85	-10.85	0	0	1.02	-4.62
4	**PQ**	0	0	0	0	1.02	-11.5
5	**PQ**	0	0	125	50	1.99	-13.27
6	**PQ**	0	0	90	30	1.01	-12.97
7	**PQ**	0	0	0	0	1.02	-5.56
8	**PQ**	0	0	100	35	1.01	-8.55
9	**PQ**	0	0	0	0	1.03	-7.31

In this test system, three machines are interconnected through a grid of nine buses, producing a total output of 319.6 MW. This output supplies an active power load of 315 MW and a reactive power load of 115 MVAR. The total losses in the transmission lines amount to 4.6 MW. Table 3 provides a summary of the data for the various nodes within the IEEE 9-Bus grid.

5.2 Analysis of Transient Stability

To assess the transient stability of the network, a three-phase fault was selected at various buses as the dynamic disturbance. This fault is applied individually at buses 4, 5, 6, 7, 8, and 9 (totaling six scenarios), and for each scenario, the critical clearing time (CCT) is calculated to evaluate transient stability. Figure 6 and Figure 7 illustrate the changes in relative angles and active power outputs of the three generators following a fault at bus 8, with a fault duration of T_d = 500 ms.

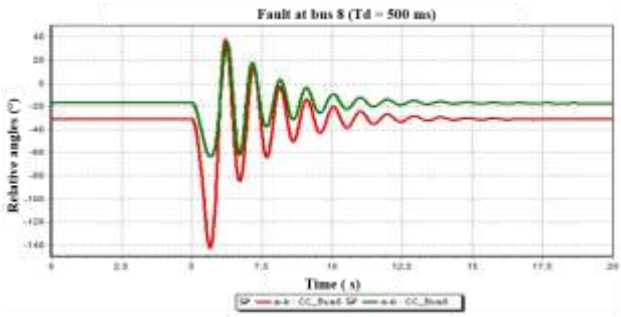

Fig. 6: Evolution of relative angles for T_d=500 ms

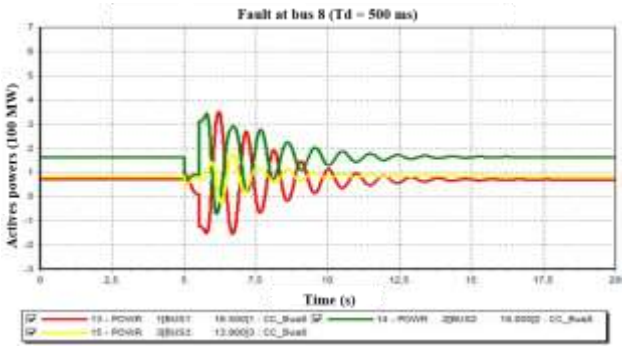

Fig. 7: Evolution of active powers for T_d=500 ms

Following a solid three-phase fault on bus 8 lasting for 500 ms, the relative angles of generators 1 and 3, as well as the active power outputs of the various generators, begin to oscillate now of the fault (t = 5s) and eventually stabilize at their initial values. These oscillations are characterized as well-damped. The maximum deviation of the relative angle for generators 1 and 3 is recorded at 140° and 65°, respectively (both less than 180°). It can be concluded that the system is in a stable state. The evolution of the relative angles for T_d = 600 ms,

corresponding to the same defect, is illustrated in Figure 8.

In the scenario where the fault duration is 600 ms, the oscillations of the various parameters remain undamped, and the relative angle of generator 1 continues to increase. This indicates that the system loses synchronization and enters a state of instability. It is observed that the critical fault clearance time lies between 500 ms and 600 ms. By varying the fault duration in increments of 10 ms and assessing the stability of the system, the critical fault clearance time is determined to be 520 ms. The same procedure was applied to other faults to ascertain the critical clearance time for each case.

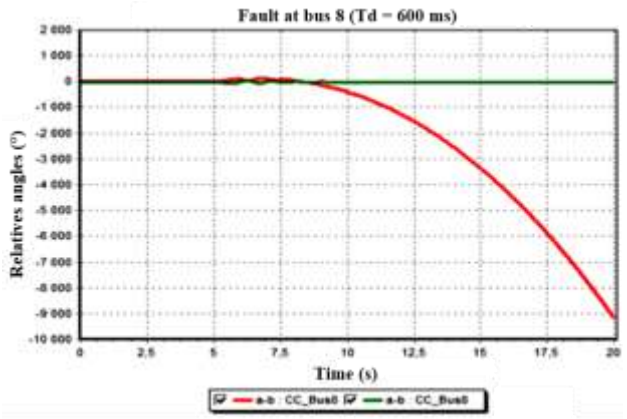

Fig. 8: Evolution of relative angles for T_d=600 ms

Table 4 summarizes the different critical clearance times and the maximum deviation of the two relative angles for each fault.

Table 4. Values of CCT and the maximum deviation angles

Fault Location	CCT (ms)	$\Delta\alpha_1$(°)	$\Delta\alpha_3$(°)
Bus 4	670	140	110
Bus 5	870	160	100
Bus 6	1100	160	140
Bus 7	260	145	90
Bus 8	520	155	90
Bus 9	410	120	160

5.3 Frequency Stability Analysis

Frequency stability refers to the ability of an electrical system to maintain a stable frequency following a significant disturbance that causes a considerable imbalance between production and consumption. To assess the frequency stability of the IEEE 9-Bus system, the frequency response of the network is analyzed, focusing on the rate of change of frequency (RoCoF) and the minimum/maximum frequency values, known as Nadir, across two power imbalance scenarios:

- Imbalance 1: Disconnection of load A (P_A=125MW; Q_A = 50 MVAR).
- Imbalance 2: Disconnection of load B (P_B=90MW; Q_B = 30 MVAR).

The evolution of bus voltages (in p.u) and the frequency response following the loss of both loads are illustrated Figure 9, Figure 10, Figure 11 and Figure 12.

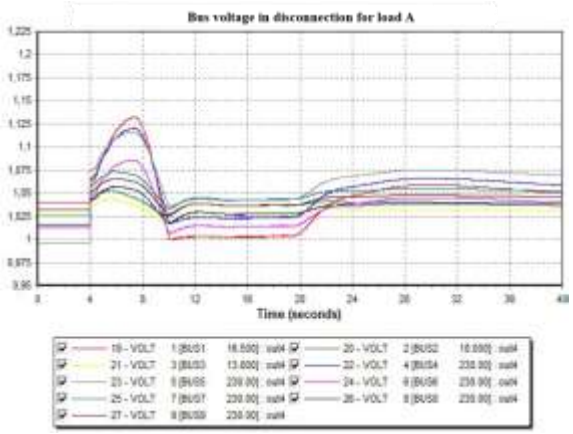

Fig. 9: Evolution of bus voltage for imbalance 1

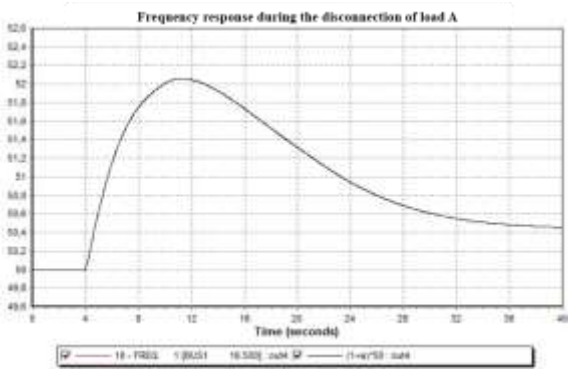

Fig. 10: frequency response for imbalance 1

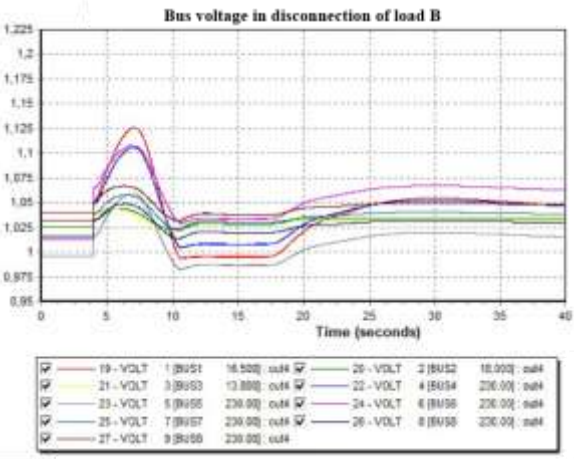

Fig. 11: Evolution of bus voltage for imbalance 2

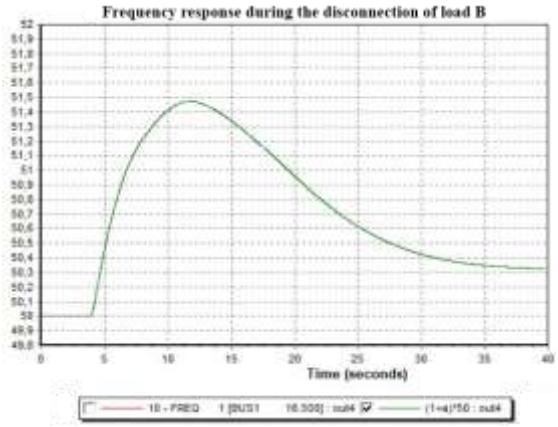

Fig. 12: frequency response for imbalance 1

In the moment of the imbalance at t = 4 s, the voltages of the various buses and the frequency begin to rise, although they do not exceed stability limits. This increase is a direct result of an imbalance between the total power generated and the total power consumed ($P_G > P_L$). Thanks to the voltage and speed regulators within the system, this rise is mitigated, and the voltage and frequency values stabilize after 30 seconds. The values of the rate of change of frequency (RoCoF) and the Nadir for each case are summarized in Table 5.

Table 5. Values of RoCoF and Nadir for imbalances 1 and 2

Imbalances	RoCoF(Hz)	Nadir (Hz/s)
1	0.6	52.05
2	0.4	51.45

According to the results, it is observed that the values of the frequency variation rate and the Nadir are higher in the case of the disconnection of load A. This indicates that the power imbalance in the first scenario is greater than in the second.

5.4 Evaluation of Grid Robustness

The robustness of the system is a common concern in the integration of renewable energy sources. This section assesses the robustness of the IEEE 9-Bus network at three different nodes (5, 6, and 8) by calculating the short-circuit ratio (SCR) to identify the most resilient location for connecting wind farms in the subsequent section. To achieve this, it is necessary to compute the apparent short-circuit power (S_{cci}) for each bus i and divide it by the active power (P_i) of the load connected to the same bus.

Table 6 summarizes the various values of the S_{cci} and SCR_i for each bus.

Table 6. Values of the Scc_i and SCR_i for each bus

Bus	Scc_i(MVA)	P_i (MW)	SCR_i
5	470	125	3.76
6	430	90	4.77
8	530	100	5.3

The SCR values can be utilized to pinpoint the weak and rigid areas within the electrical system. It is observed that, in the IEEE 9-Bus network, bus 8 is the most robust, exhibiting the highest SCR value when compared to buses 5 and 6.

6 Impacts of Wind Turbine Integration

6.1 Effects of the Interconnection Point's Robustness on the Transient Stability

To assess the influence of the interconnection point's robustness on the transient stability of the grid, a 50 MW wind farm is connected under two distinct scenarios:

- Case 1: A wind farm with a capacity of 50 MW is connected to node 8 ($SCR_8 = 5.3$).
- Case 2: A wind farm with a capacity of 50 MW is connected to node 5 ($SCR_5 = 3.76$).

The critical clearing times (CCT) for fault elimination are calculated for each case, followed by a comparison of the results obtained. In the base state of the network, without the connection of the wind farm, the CCT values vary depending on the type of fault. When the wind farm is connected to the network at bus 8 or bus 5, the CCT values decrease, resulting in less time for the grid to respond before entering a state of instability.

The CCT values for each scenario baseline, Case 1, and Case 2 are summarized in Table 7.

Table 7. Comparison of CCT values for the cases: baseline, 1, and 2

Fault location	CCT base case(ms)	CCT Case 1(ms)	CCT Case 2(ms)
Bus 4	670	560	420
Bus 5	870	700	320
Bus 6	1100	980	950
Bus 7	260	150	140
Bus 8	520	220	300
Bus 9	410	300	280

Based on the results obtained, it is observed that the CCT values for case 2 are all lower than those for case 1, except for the fault in bus 8 where the

wind turbine is connected. These findings indicate that as the short-circuit ratio (SCR) at the interconnection point of the renewable energy source (RES) decreases, the CCT values also decrease, thereby adversely affecting the transient stability of the network.

6.2 Effect of Total System Inertia on RoCoF

To assess the impact of reduced total system inertia (Hsys) on the frequency stability of the network, one of the two generators, 1 or 3, which have different inertia constants, is replaced with a MADA wind farm of equivalent power. Subsequently, the other synchronous generator is lost, and the frequency response is evaluated, followed by the calculation of the RoCoF values obtained for both scenarios.

- Case 1: The synchronous machine 1 (H_1=9.55 s) is replaced with a wind turbine of equivalent power (72 MW), followed by the disconnection of synchronous machine 3.
- Case 2: The synchronous machine 3 (H_3=2.35 s) is replaced with a wind turbine of equivalent power (85 MW), followed by the disconnection of synchronous machine 1.

The frequency response for Case 1 and Case 2 are illustrated in Figure 13 and Figure 14, respectively.

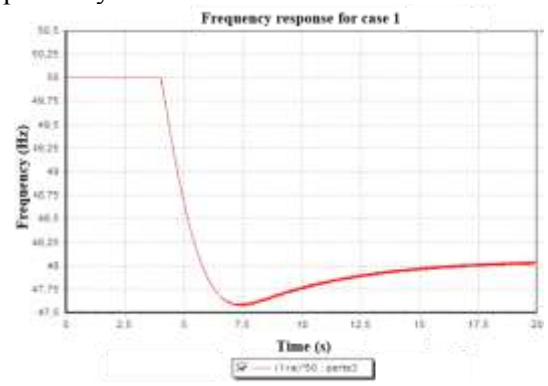

Fig. 13: Frequency response for case 1

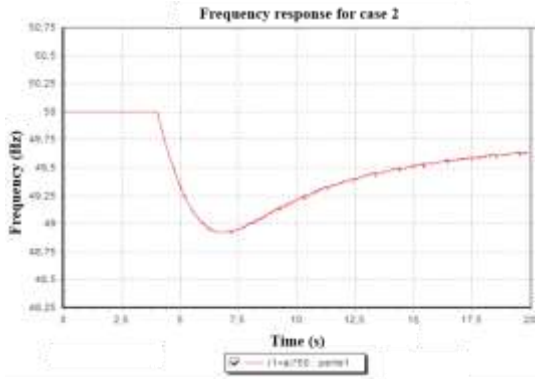

Fig. 14: Frequency response for case 2

In both simulation scenarios, following the disconnection of a synchronous generator at t=4 s, the frequency of the grid begins to decline for a duration of 2 to 3 seconds after the fault occurs, ultimately reaching its lowest point, referred to as the Nadir. The graphically calculated RoCoF values and the Nadir for each case are compiled in Table 8.

Table 8. Comparison of RoCoF and Nadir values obtained for cases 1 and 2.

	RoCoF(Hz)	Nadir (Hz)
Case 1	1.25	47.6
Case 2	0.85	48.9

It is observed that $RoCoF_1$ is greater than $RoCoF_2$, while $Nadir_1$ is less than $Nadir_2$. This indicates that the frequency variation, primarily caused by the power imbalance, is more significant in case 1. To explain this difference in the frequency responses of the system, the total inertia of the system is calculated for each case based on equation 7.

$$H_{sys1} = \frac{(3.33\times3.10)+(2.35\times2.80)}{260+310+280} = 1.99\ s \qquad (12)$$

$$H_{sys2} = \frac{(9.55\times2.60)+(3.33\times3.10)}{260+310+280} = 4.14\ s \qquad (13)$$

The replacement of the generator with the highest inertia by a wind farm of equivalent capacity (case 1) results in a significant reduction of the total system inertia (Hsys 1 = 1.99 s), which subsequently leads to an increase in the rate of change of frequency (RoCoF).

It is further confirmed that as the total system inertia decreases ($H_{sys1} < H_{sys2}$), the value of RoCoF increases ($RoCoF_1 > RoCoF_2$).

Based on the results obtained, the following conclusions can be cited:

- ✓ Conventional generators store kinetic energy within their rotating components.
- ✓ The stored kinetic energy is released or absorbed directly in response to a disturbance, thereby enhancing the initial frequency response of the system.
- ✓ The transition from conventional generators to wind farms has resulted in a reduction in system inertia and a deterioration of frequency stability.
- ✓ The significance of the location of these wind farms cannot be overlooked.
- ✓ Most renewable energy sources installed far from the main grid have weak and insufficiently robust connection points, leading to a decline in transient stability (reduction in CCT) and voltage stability.

7 Conclusion

In this study, we conducted an analysis of the effects of integrating wind energy sources on the frequency stability of the electrical grid, utilizing a set of indicators to assess grid stability and robustness. We began our investigation with a brief overview of electrical grid stability and the challenges posed by the integration of renewable energy sources.

These resources have limited participation in frequency and voltage control services. Regulatory requirements for their integration (GCR) are established by electrical network operators. In the second section, we presented various stability indicators (critical clearing time, inertia, and rate of change of frequency) along with different methods for evaluating network robustness (SCR, WSCR, and CSCR). Simulations conducted on the IEEE 9-Bus grid revealed the various impacts associated with the integration of wind farms and demonstrated the influence of system inertia and the robustness of the connection point on stability indicators. The simulation results indicate that an increase in the penetration rate of wind turbines in the grid leads to negative impacts on CCT, RoCoF, Nadir, and SCR parameters. This is attributed to a reduction in overall inertia. To mitigate these impacts, it is necessary to reassess the triggering thresholds of various protections, their selectivity, and the RoCoF thresholds used in the load-shedding plans of the electrical grid.

Declaration of Generative AI and AI-assisted Technologies in the Writing Process

The authors wrote, reviewed and edited the content as needed and they have not utilised artificial intelligence (AI) tools. The authors take full responsibility for the content of the publication.

References:

[1] S. Saha, M.I. Saleem, T.K. Roy. Impact of high penetration of renewable energy sources on grid frequency behavior, *International Journal of Electrical Power & Energy Systems*, Vol. 145, February 2023, 108701. https://doi.org/10.1016/j.ijepes.2022.108701.

[2] F. Gonzalez-Longatt, J.M. Roldan-Fernandez, H.R. Chamorro, S. Arnaltes, J.L. Rodriguez-Amenedo, Investigation of inertia response and rate of change of frequency in low rotational inertial scenario of synchronous dominated system, *Electronics*, Vol. 10, No. 18, 2021, pp. 2288. https://doi.org/10.3390/electronics10182288.

[3] D. Jayaweera, *Smart Power Systems and Renewable Energy System Integration,* Springer International Publishing, 2016. DOI: 10.1007/978-3-319-30427-4.

[4] H. Golpîra, A. Román-Messina, H. Bevrani, Renewable Integrated Power System Stability and Control, *Wiley-IEEE Press,* April 2021, ISBN: 978-1-119-68979-9.

[5] M. El-Shennawy, S. Farghal, A. E. Amin, S. Abdelkader, Impact of Renewable Energy Sources on Inertia and Frequency Response of Power Systems, *Mansoura Engineering Journal*, Vol. 43, No. 3, 2020, Article 12. DOI: 10.21608/bfemu.2020.95749.

[6] ENTSO-E, Determining Generator Fault Clearing Time for the Synchronous Zone of Continental Europe - Version 1.0, RG-CE *System Protection & Dynamics Sub Group*, 3 February 2017, pp.1-15, [Online]. https://www.entsoe.eu/Documents/2017/SP (Accessed Date: November 3, 2024).

[7] P. Tielens, P. Henneaux, S. Cole. Penetration of renewables and reduction of synchronous inertia in the European power system - Analysis and solutions, *Engineering, Environmental Science*, 2018, pp. 9-10.

[8] J. Beyza, J.M. Yusta. The effects of the high penetration of renewable energies on the reliability and vulnerability of interconnected electric power systems, *Reliability Engineering & System Safety*, Vol. 215, November 2021, 107881. https://doi.org/10.1016/j.ress.2021.107881.

[9] P. Tielens, D. Hertem. Grid inertia and frequency control in power systems with high penetration of renewables. *Engineering, Environmental Science*, Avril 2012, pp. 1-5.

[10] M.D. Shafiul Alam, Fahad Saleh Al-Ismail, Aboubakr Salem, and Mohammad A. Abido, High-Level Penetration of Renewable Energy with Grid: Challenges and Opportunities, *IEEE Access,* Vol. 8, 29 October 2020, pp. 170831-170845. DOI: 10.48550/arXiv.2006.04638.

[11] Partha P. Biswas, Parul Arora, R. Mallipeddi, P. N. Suganthan, and B. K. Panigrahi, Optimal placement and sizing of FACTS devices for optimal power flow in a wind power integrated electrical network, *Neural Computing and Applications,* Vol. 33, 5 November 2020, pp. 6753–6774, 2021.

Contribution of Individual Authors to the Creation of a Scientific Article (Ghostwriting Policy)

The authors equally contributed in the present research, at all stages from the formulation of the problem to the final findings and solution. Specifically:

- Laila Bouaziz carried out the theoretical modeling and simulation analysis.
- Mehdi Dhaoui supervised the data analysis and provided overall technical guidance.
- Mouna Ben Hamed contributed to the manuscript writing and critical review.

Sources of Funding for Research Presented in a Scientific Article or Scientific Article Itself

No funding was received for conducting this study.

Conflict of Interest

The authors have no conflicts of interest to declare.